Pricing electricity in constrained networks dominated by stochastic renewable generation and electric energy storage

Per Aaslid [*,a,b], Magnus Korpås [b], Michael M Belsnes [a], Olav B Fosso [b]

[a] SINTEF Energy Research, Trondheim, Norway
[b] Norwegian University of Science and Technology, Department of Electric Power Engineering, Trondheim, Norway

ARTICLE INFO

ABSTRACT

This paper studies the electricity price formation in a competitive market when introducing generation from variable renewable energy technologies with zero marginal cost and electric energy storage systems. A power system is analyzed with a stochastic optimization model combining multi-period optimal power flow with stochastic dynamic programming. The results illustrate how variable renewable energy, in this case solar photovoltaic generation, displaces some of the expensive thermal generation and reduces the price. Electric energy storage will reduce the price variations caused by the variable renewable generation and demand as the time with price cap and zero price is reduced. In systems with only variable renewable generation and energy storage, the price will be set by the probability of scarcity similar to the price formation in hydro power dominated systems. The price will indicated the future cost of scarcity as a stochastic expectation value. This paper assumes that the demand is inflexible. However, the resulting electricity prices will remunerate provision of flexibility, which in turn will contribute to securing the supply and reducing the price volatility.

1. Introduction

The share of Variable Renewable Energy (VRE) generation worldwide is increasing, and although most electricity markets still are dominated by thermal generation, projections show that VRE will be the dominant energy source by 2050 both in terms of electricity generation and and installed capacity [1]. Until now, the deployment of VRE has to a large extent been driven by subsidies, but the cost level of VRE has been decreasing rapidly and is now becoming lower than conventional generation, even without subsidies [2].

VRE has a marginal operating cost close to zero and will therefore displace some of the dispatchable generation due to the merit order effect, which has been extensively studied [3–8]. This in turn will reduce the profit of the conventional generation units, but also make large-scale deployment of competitive VRE more difficult due to the energy price reduction [9]. However, Helm and Mier [10] shows that VRE can be competitive in an energy-only market when the levelized cost of energy is sufficiently low. Moreover, Korpås and Botterud [11] show that there exists a market equilibrium including VRE in an energy-only market where all units recover their costs. The market price at the new equilibrium will be more volatile compared to a system without VRE. The

new market equilibrium will also have a significant duration of zero price, a higher amount of energy not supplied, and there will be relatively more power stations with higher variable costs and lower fixed costs [12].

Electric Energy Storage (EES) can facilitate integration of VRE. The deployment of grid scale EES has seen a tremendous growth since 2013 [13], partly driven by decreasing EES costs [14]. The application of EES in combination with VRE has been extensively studied [15,16], either from a system optimization perspective [17,18], or from a price taker perspective [19,20] regardless of generating source. The EES profit in a wholesale market comes from arbitrage, hence accurate price forecasts capturing both the volatility as well as the uncertainty are important. Ward et al. [21] shows that current market models tend to underestimate the volatility, and suggests a more accurate description of the merit order to better capture the price volatility and to account for the implications on the market equilibrium caused by EES by solving the model iteratively. The implications EES have for the market equilibrium are studied more in detail in Korpås and Botterud [11] where they show how profit maximization for each generation and storage unit in a market based on marginal cost pricing and administrative scarcity pricing will have the same result as system cost minimization using traditional system optimality and cost recovery conditions from Stoft

---

Nomenclature

Sets and indices

$b \in \mathscr{B}$ Set of buses in network

$(i,k) \in \mathscr{L}$ Set of lines in network

$(i,k) \in \mathscr{L}_b$ Set of lines from bus b

$s \in \mathscr{S} = [1, S]$ Set of stages in optimization problem

$t \in \mathscr{T}_s = \left[\underline{t}_s, \bar{t}_s \right]$ Set of time steps at stage s

$n \in \mathscr{N} = [1, N]$ Set of discrete states at each stage

$\omega_s \in \Omega_s$ Noise in sample space at stage s

$m \in \mathscr{M}$ Set of discrete scenarios from noise probability distribution

$e \in \mathscr{E}_b$ Set of EES at bus b

$g \in \mathscr{G}_b$ Set of thermal generation units at bus b

$r \in \mathscr{R}_b$ Set of VRE generation units at bus b

$d \in \mathscr{D}_b$ Set of loads at bus b

Parameters

P_g^{max} Maximum active power for thermal generator g

$P_{r,t}^{max}$ Theoretical maximum generation solar power system r, time t

$\phi_{r,s}$ Clearness index solar power system r, stage s

ρ_m Noise probability scenario m

$PD_{d,t}$ Active power demand forecast load d, time t

B_{ik} Imaginary component of admittance matrix element ik

$\Theta_b^{min}/\Theta_b^{max}$ Minimum/maximum voltage angle at bus b

P_{ik}^{max} Maximum transmission capacity for line between bus i, k

C_g Generator g marginal operating cost

C_d Load d marginal shedding cost

X_n Discrete state n

ΔT_t Step length at time t

SOC_e^{min}/SOC_e^{max} Minimum/maximum SOC at storage e, time t

$PS_{e,t}^c/PS_{e,t}^d$ Maximum charge/discharge power at storage e, time t

$\beta_{q,s,n}$ Spline coefficient order q, discrete state n at stage s

η^c/η^d EES charge/discharge efficiency

Variables and Functions

x_s/x_s' Incoming/outgoing state variables at stage s

$\bar{x}_s$ Incoming state dummy variable at stage s

u_s Control variable at stage s

$U_s(x_s, \omega_s)$ Control variable feasibility set at stage s

$T_s(x_s, u_s, \omega_s)$ Stage-transition function between stage s and $s+1$

$C_s(x_s, u_s, \omega_s)$ Stage-objective function at stage s

$V_s(x_s, \omega_s)$ Future cost function at stage s

$\pi_s(x_s, \omega_s)$ Decision-rule function at stage s

$\lambda_{s,n}$ State variable dual value at stage s, discrete state n

$p_{b,t}$ Active power injection at bus b, time t

$p_{g,t}$ Active power thermal generator g, time t

$p_{r,t}$ Active power from solar power system r, time t

$p_{e,t}$ Active power withdrawn by storage e, time t

$ps_{e,t}$ Net power charged to storage e

$ps_{e,t}^c/ps_{e,t}^d$ Power charged to/discharge from storage e, time t

$soc_{e,t}$ Energy storage e SOC, time t

$p_{d,t}$ Active power withdrawn by load d, time t

$pls_{d,t}$ Shedding of load d, time t

$\theta_{b,t}$ Voltage angle at bus b, time t

$SEV_s(x_s)$ Storage end value function at stage s

$SMV_s(x_s)$ Storage marginal value function at stage s

sev_s Storage end value variable at stage s

$B_{q,s,n}(x_s)$ Spline order q, discrete state n at stage s

$\Pi_n(x_s)$ Spline activation function discrete state n

---

[22]. Since the approach is based on duration curves, the storage size limitations are not accounted for.

The similarities between the hydro power dominated electricity markets, such as the Nordic market, and markets with high penetration of VRE and EES, are interesting when studying the market equilibrium and the corresponding electricity prices. The marginal cost pricing principle is also used in these markets [23], and the marginal value for hydro power plants has been studied for decades [24]. In contrast to VRE and thermal generation, the marginal value for a hydro power plant is not given by its operational costs but the future opportunity value of saving the stored energy for later rather than using it now [25].

The marginal value of EES, hereby referred to as the Storage Marginal Value (SMV), is actually a function of both time, due to variations in generation and demand, and EES State-Of-Charge (SOC) as the capacity for avoiding expensive generation or load curtailment in the future depends on the current SOC. The SMV will therefore also be a function of the SOC of other EES' in the system [26] since the risk of scarcity depends on the total energy stored in the system and potential grid congestion associated with the EES locations. Although the proposed method supports multiple EES [27], this paper will study a single aggregated storage. Moreover, both generation from VRE and demand are subject to uncertainty. Seen from a system perspective, the future SOC depends on the realizations of the uncertainty and will therefore also influence the future electricity price. Since the operation strategy may be corrected multiple times as the uncertainty is revealed, the problem is tractable to formulate as a multi-stage stochastic model. Geske and Green [28] points out that if EES capacity replaces some generation capacity, the optimal EES strategy must balance arbitrage against the risk of not being able to meet the system demand. The electricity price can in this case be seen as an arbitrage against risk of extreme prices.

The implications on electricity prices caused by large-scale integration of VRE and EES have until now been studied for systems where dispatchable generation technologies are still the backbone of the electricity system. This paper goes one step further and analyses the implications on a power system when VRE is the dominating source of power generation, and the system relies on EES to secure the supply.

This paper presents a multi-stage stochastic optimization model of an electricity system with VRE and EES seen from a system perspective and solves it with Stochastic Dynamic Programming (SDP) [29]. The model formulation is based on Multi-Period Optimal Power Flow (MP-OPF) [30].

The solution of the model yields the SMV for all time steps as a function of SOC as a cubic spline function. The SMV indicates the operating strategy for that particular EES in a wholesale market. Moreover, by simulating several scenarios sampled from the probability distribution, a range of possible electricity prices can be generated yielding a probabilistic electricity price for all buses in the entire system. The resulting electricity price will be studied to illustrate the effect of introducing VRE and EES in a power system dominated by thermal generation, thus confirming the results from previous studies and the correctness of the proposed model. Finally, the electricity price in a system with only VRE and EES will be studied where the price is set by the risk of extreme prices caused by scarcity.

The contributions of this paper can be summarized as follows:

i) A novel SDP model for electricity system optimization including EES and uncertainty. The model embeds MP-OPF as stage-wise models, and connects them through cubic spline end value functions generated from the state variable dual values.

ii) The storage end value for the final stage is updated iteratively to simulate infinite horizon optimization.

iii) The electricity price is studied first for a traditional power system with thermal generation, followed by systems including VRE and EES. Finally, the price is studied for a system with only VRE and EES.

iv) The interpretation and usage of the storage marginal value function are discussed.

The remainder of this paper is organized as follows: Section 2 describes the optimization method used to find the SMV and Locational Marginal Price (LMP), Section 3 presents numerical data used to illustrate the energy price in a system dominated by thermal generation compared to VRE generation, Section 4 presents the results using the described method in combination with the presented numerical data, Section 5 discusses the implications of the presented results, and Section 6 draws the conclusions and presents possible directions for future work.

2. Method

This section presents a detailed description of the multi-stage stochastic optimization problem used to study the optimal operation and the corresponding electricity price in a constrained power system with VRE generation and EES under uncertainty, exemplified by the system in Fig. 1. The presented solution method combines SDP and MP-OPF.

2.1. Multi-stage stochastic programming

The goal with the proposed optimization problem is to find the optimal operation of generators, EES and loads, and to study the resulting LMP and SMV. The objective is to minimize operation costs. The ability to deliver and absorb energy from an EES depends on its SOC, and the SOC depends on the operation strategy and the realization of uncertain variables. The SOC and other variables coupled in time, hereby referred to as state x_s, will therefore require additional attention. Due to uncertainty in generation and load, the resulting operation strategy of a deterministic model formulation will often in practice be sub-optimal, and could even be infeasible due to the differences in the predicted and the actual generation and load. A more robust and realistic approach is to assume the uncertainty is revealed stage-wise as time elapses, and that the operation strategy also can be corrected stage-wise as more uncertainty becomes known. These assumptions makes the problem tractable to formulate as a multi-stage stochastic optimization problem.

The following stochastic programming terminology is based on Dowson [31]. Instead of solving the stochastic optimization problem as one large problem, it is broken down into a sequence of smaller stage-wise problems. Each stage $s \in \mathscr{S}$ represents a discrete moment in time where uncertainty is revealed and a decision is made. The stage objective represents the operation costs, such as generation and load shedding costs. The decision process for each stage is illustrated in Fig. 2, where the decision-rule $\pi_s(x_s, \omega_s)$ chooses a control u_s that respects the set of admissible controls such that $u_s \in U_s(x_s, \omega_s)$. The overall goal is to find a policy, a sequence of decision-rules $\pi = \{\pi_1, \cdots, \pi_S\}$, that minimizes the sum of all the stage objectives $C_s(x_s, u_s, \omega_s)$.
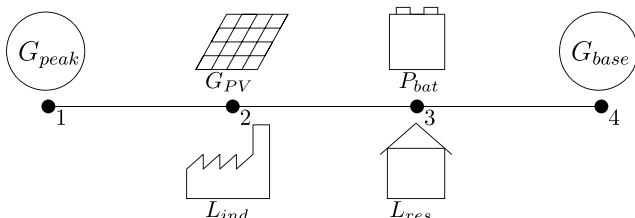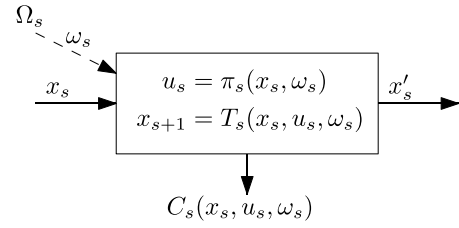

Fig. 2. Multi-stage stochastic optimization decision node [31]

The stages divide the full problem into smaller sub-problems in a similar manner as continuous time problems are divided into discrete time steps. The time between stages, the stage length, is a compromise between accuracy and computational burden but should also reflect how the system is operated. Hourly stages could be a good choice when operating in an hourly market, but the EES size and the noise variability are also important factors. At each stage, the noise $\omega_s \in \Omega_s$ is observed and assumed to be known for that stage. The noise represents the uncertainty in VRE generation, but may also include load uncertainty, and describes the possible variability in energy delivered by VRE due to uncertainty. The perfect foresight assumption for the current stage can be justified through accurate short-term forecasts and that the uncertainty has only a relatively small impact on the state for a single stage.

The noise in the model formulation should be stage-wise independent, signifying that the observed noise at a stage does not influence the noise in the next stage. In other words, if it is more sunny than expected at one stage such that the VRE generation is increased, it will not influence the probability of increased generation at the next stage. This assumption might be inaccurate and could be compensated for by including the VRE generation in the state with, for example, an autoregressive model [32,33].

For this particular system, the state is given by the EES SOC. The capability of delivering energy from the EES depends on sufficiently high SOC, and the capability of absorbing energy depends on sufficiently low SOC. In contrast, dispatchable generators can freely change the generation independent of generation in the previous stage (unless ramping limitations must be accounted for).

The control variable represents all the decisions made to balance generation and load, such as how much the different generators should deliver, and how much the EES should deliver or absorb. VRE generation curtailment and load shedding are also decisions in the control variable. All these decisions must be admissible $u_s \in U_s(x_s, \omega_s)$ such that that generation minimum and maximum limits, EES charge/discharge limits, load shedding limits and generation curtailment limits are respected, and the network is not overloaded.

The transition function $T_s(x_s, u_s, \omega_s)$ describes how the state evolves for a given control and observed noise, in this case how the EES SOC changes given the decisions for how to meet the load and the observed generation for the current stage. The stage-objective $C_s(x_s, u_s, \omega_s)$ represents the corresponding operation costs related to generation costs and load shedding.

2.2. Stochastic dynamic programming

According to Bellman's principle of optimality [29], the optimal policy can be found by solving the optimization problem recursive. By assuming the future optimal decisions are known, the optimal decision for the current stage can also be found. Moreover, the entire problem can then be solved with backward recursion. The resulting recursive optimization problem is shown in Eq. 1.

$$
\begin{aligned}
V_s(x_s, \omega_s) &= \min_{u_s}\left\{ C_s(x_s, u_s, \omega_s) + \underset{\omega_{s+1}\in\Omega_{s+1}}{\mathbb{E}}\left[V_{s+1}\left(x_s', \omega_{s+1}\right)\right]\right\} \\
\text{s.t.}\quad x_s' &= T_s(x_s, u_s, \omega_s) \\
u_s &\in U_s(x_s, \omega_s)
\end{aligned}
\tag{1}
$$

Fig. 1. Power system topology.

This problem will be solved with a SDP method called the water value method from hydro power optimization [25]. The expectation of the future costs is replaced with the Storage End Value (SEV) as shown in Eq. 2.

$$
\begin{aligned}
\min_{u_s}\{&C_s(x_s, u_s, \omega_s) - sev_{s+1}\} \\
\text{s.t. } x_s' &= T_s(x_s, u_s, \omega_s) \\
sev_{s+1} &\leq SEV_{s+1}(x_s') \\
u_s &\in U_s(x_s, \omega_s)
\end{aligned}
\tag{2}
$$

The objective function of the presented optimization problem in Eq. 2 has a very interesting structure. The first term represents the operational costs of the current stage, often referred to as the immediate costs, while the second term represents the SEV and is a function of the outgoing state. Just like the generation marginal cost C_g is given by the derivative of the cost function with respect to the generation p_g Eq. 3, the marginal value of the state (here SOC) is given by the derivative of the SEV function with respect to the state Eq. 4. Numerical examples in Section 4 will provide a clearer understanding of the relation between SMV, generator marginal cost and their applications.

$$
C_g = \frac{dC}{dp_g}
\tag{3}
$$

$$
SMV_s(x_s) = \frac{dSEV_s(x_s)}{dx_s}
\tag{4}
$$

However, the marginal value of the state is a function of both state and stage. In other words, the marginal value of the EES depends on its SOC and stage due to the variability in future expected generation and load. Since it is difficult to solve the optimization problem with respect to a continuous state variable x, it is discretized into N discrete states. Each stage-wise optimization problem is solved for each discrete state $n \in \mathcal{N}$ and each scenario $\omega_s \in \Omega_s$. The solution of the optimization problems forms the basis for approximating the SEV function. This approximation is described in Section 2.3, and a procedure for finding the SEV for the final stage is described in Section 2.3.1. The SEV function $SEV_s(x_s)$ is convex if the sub-problem given by $C_s(.), T_s(.), U_s(.)$ is convex in x_s, ω_s and is therefore expressed as a convex relaxation in Eq. 2 (although SDP also permits non-linear sub-problems).

2.3. Storage end value function

The SEV function will be expressed as a cubic spline function yielding a smooth function, as illustrated in Fig. 3, demanding fewer discrete states than a piece-wise linear approximation [27]. A spline function is a piece-wise polynomial function composed of polynomials up to degree q
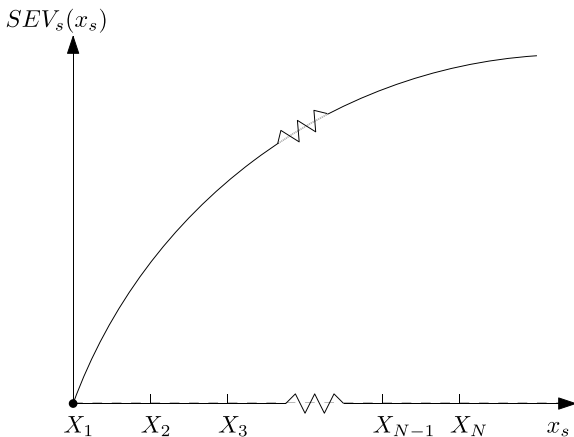

Fig. 3. Storage end value function.

with continuous derivatives up to the order $q - 1$. A cubic spline will therefore have piece-wise cubic segments, and continuous derivatives up to the order of two. This makes it possible to embed the SEV function into a non-linear optimization problem where all the constraints and the objective must be twice continuously differentiable in order to solve the problem with interior point based methods.

The SEV function is approximated using the marginal value given by the dual value of the state x. The initial value of the SEV function can also be chosen arbitrarily and is set to zero such that the SEV of empty storage is zero. By adding the dummy variable $\bar{x}_s$ and the constraint Eq. 5 to the optimization problem in Eq. 2, the corresponding dual variable λ_s will represent the marginal value of SEV function with respect to the state x [34]. Let λ_{s,n,ω_s} denote the dual value at stage s for the discrete state n and the noise ω_s such that the expected dual value $\lambda_{s,n}$ for stage s and discrete state n is given by Eq. 6.

$$
x_s = \bar{x}_s, \quad | \quad \lambda_s
\tag{5}
$$

$$
\lambda_{s,n} = \mathop{\mathbb{E}}_{\omega_s \in \Omega_s}\left[\lambda_{s,n,\omega_s}\right]
\tag{6}
$$

The SEV function Eq. 7 is expressed as a sum of polynomials Eq. 8 multiplied with an activation function Eq. 9 defined such that the correct spline segment is activated.

$$
SEV_s(x_s) = \sum_{n=1}^{N-1} B_{q,s,n}(x_s)\, \Pi_n(x_s),
\tag{7}
$$

$$
B_{q,s,n}(x_s) = \sum_{\eta=0}^{q} \beta_{\eta,s,n}(x_s - X_n)^\eta,
\tag{8}
$$

$$
\Pi_n(x_s) = \begin{cases} 1, & \text{if } X_n \leq x_s < X_{n+1} \\ 0, & \text{otherwise} \end{cases} \\ s \in \mathcal{S}, n \in \mathcal{N}\backslash\{N\}
\tag{9}
$$

Each spline segment Eq. 8 of a cubic spline is uniquely defined by the four coefficients $\beta_{\eta,s,n} \mid \eta \in [0, q]$. If spline segment n is known, then the value and derivatives up to order two of segment $n + 1$ are also given at the intersection between segment n and $n + 1$. Therefore, segment $n + 1$ has only one degree of freedom and can be fitted using the derivative at the next intersection. The initial value of the first segment and and the initial second order derivative is also assumed to be zero. The spline function can therefore be found by solving the set of equations in Eq. 10.

$$
\begin{aligned}
B_{3,s,1}(0) &= 0, \\
B_{3,s,1}''(0) &= 0, \\
B_{3,s,n}'(X_n) &= \lambda_{s,n} \\
B_{3,s,n}(X_{n+1}) &= B_{3,s,n+1}(X_n) \\
B_{3,s,n}'(X_{n+1}) &= B_{3,s,n+1}'(X_n) \\
B_{3,s,n}''(X_{n+1}) &= B_{3,s,n+1}''(X_n) \\
s &\in \mathcal{S}, \ n \in \mathcal{N}\backslash\{N\}
\end{aligned}
\tag{10}
$$

2.3.1. Storage end value boundary conditions

The presented storage optimization problem has in reality infinite horizon. Stage s in the SDP algorithm uses the SEV function generated in stage $s + 1$ as the boundary condition for the stage-wise optimization problem. The final stage, which is optimized first due to the backward recursion, does not have any SEV function generated by the subsequent stage. If the SEV at the end of the final stage is not properly defined, the storage will typically be emptied. The end state can also be bounded by a fixed value [35–37]. However, this paper proposes an iterative SEV update procedure to approximate the SEV at the end of the final stage. The SEV function for the final stage is initially estimated by assuming that the slope equals the value of lost load for minimum SOC and the slope is zero for maximum SOC. The SEV function at the final stage is thereafter updated iteratively with the SEV function from the first stage until the solution converges. This is equivalent to solving the problem repeatedly such that the choice of final end value does not influence the

solution, and could be considered as equivalent with infinite horizon [25].

2.4. Multi-period optimal power flow

The stage-wise optimization problem Eq. 2 is given by a MP-OPF problem. The incoming state is given by the initial SOC and the outgoing state by the end SOC as shown in Eq. 11 and 12.

$$x_s = \left\{ soc_{e,\underline{t}_s} \right\} \tag{11}$$

$$x'_s = \left\{ soc_{e,\overline{t}_s} \right\} \tag{12}$$
$$\forall e \in \mathscr{E}_b, b \in \mathscr{B}$$

All other variables are control variables, either given explicitly such as the generation, or implicitly like the bus voltage angle that follows from the other decisions as shown in Eq. 13. Moreover, the SOC variables not part of the state are included here and have therefore been assigned to a different subset of the time steps denoted $\widetilde{t}$ in Eq. 13.

$$u_s = \left\{ p_{b,t}, p_{g,t}, p_{r,t}, p_{e,t}, ps^c_{e,t}, ps^d_{e,t}, p_{d,t}, pls_{d,t}, soc_{e,\widetilde{t}}, \theta_{b,t} \right\}$$
$$\forall b \in \mathscr{B}, g \in \mathscr{G}_b, r \in \mathscr{R}_b, e \in \mathscr{E}_b, d \in \mathscr{D}_b, t \in \mathscr{T}_s, \widetilde{t} \in \mathscr{T}_s \backslash \left\{ \underline{t}_s, \overline{t}_s \right\}$$
$$\tag{13}$$

Finally, the noise of this model is the clearness index (CI) as shown in Eq. 14. The relation between CI and generation is described in Section 2.4.1, and a comprehensive introduction to CI is given in Section 2.5.1. The CI is sampled from a beta distribution, as described in Section 2.5.2.

$$\omega_s = \left\{ \phi_{r,s} \right\} \quad \forall r \in \mathscr{R}_b, b \in \mathscr{B} \tag{14}$$

2.4.1. Power flow

The power flow equations describe the relation between bus power injections and voltages at buses in a power system and form the key constraints for the Optimal Power Flow (OPF) optimization problem. All the power flow equations are included in the set of admissible control $U_s(x_s, \omega_s)$.

There exist many different OPF formulations, both exact models, approximations and relaxations, and they can be expressed in terms of bus injections or branch flows [38,39] either in rectangular or polar form [40]. The AC-OPF [41] provides an exact solution for the OPF problem, but due to the non-convex nature of the power flow equations, a global optimal solution cannot be guaranteed. The DC-OPF is linear, and derived by neglecting the line resistance and reactive power, assuming unity voltage magnitude and small voltage angles. The method is computationally efficient, easy to implement and widely used, but must be used carefully as it can deviate significantly from AC-OPF on constrained lines and therefore give inaccurate LMP [42].

To also account for the dynamic behavior of energy storage, the OPF formulation is repeated for each time step, and energy storage equations are included yielding the multi-period OPF.

This paper will use the DC MP-OPF, but the proposed method will work for any convex MP-OPF formulation. The DC power flow neglects the line resistance and assumes small voltage angles such that $\sin(\theta_i - \theta_k) \approx \theta_i - \theta_k$. The resulting bus power injections are given by Eq. 15, the line power is bounded by Eq. 16 and the voltage angle must stay within its limits Eq. 17.

$$p_{b,t} = \sum_{(i,k) \in \mathscr{L}_b} B_{ik} \left(\theta_{i,t} - \theta_{k,t} \right) \tag{15}$$

$$-P^{max}_{ik} \leq B_{ik} \left(\theta_{i,t} - \theta_{k,t} \right) \leq P^{max}_{ik} \tag{16}$$

$$\Theta^{min}_b \leq \theta_{b,t} \leq \Theta^{max}_b \tag{17}$$

To balance generation and load, the bus power injection is given by the sum of generation from both thermal and renewable generators minus loads and energy storage charging for all the units on the respective bus Eq. 18.

$$p_{b,t} = \sum_{g \in \mathscr{G}_b} p_{g,t} + \sum_{r \in \mathscr{R}_b} p_{r,t} - \sum_{e \in \mathscr{E}_b} p_{e,t} - \sum_{d \in \mathscr{D}_b} p_{d,t} \tag{18}$$

The thermal generation must not exceed its maximum generation and can be operated continuously from zero to maximum Eq. 19. The VRE generation is shown in Eq. 20. The maximum VRE generation is time dependent and is bounded by the theoretical maximum $P^{max}_{r,t}$ multiplied by a scale factor sampled from the uncertainty distribution and is further described in Section 2.5.1. Note that this representation of uncertainty is specific for solar PV generation. The load can be curtailed where the cost is given by the scarcity price Eq. 21.

$$0 \leq p_{g,t} \leq P^{max}_g \tag{19}$$

$$0 \leq p_{r,t} \leq \phi_{r,s} \cdot P^{max}_{r,t} \tag{20}$$

$$p_{d,t} = PD_{d,t} - pls_{d,t} \geq 0 \tag{21}$$

2.4.2. Electric energy storage

The EES SOC at a time step equals the SOC at the previous step plus the power charged $ps^c_{e,t}$ minus the power discharged $ps^d_{e,t}$ compensated for the efficiency losses η^c, η^d that includes both converter and battery losses Eq. 22. The power withdrawn from the bus equals the power charged minus the power discharged Eq. 23, and the energy storage upper and lower bounds are enforced by Eq. 24. The EES maximum charge and discharge power due to, for example, converter and battery limitations are enforced by Eq. 25 and 26.

$$soc_{e,t} = soc_{e,t-1} + \Delta T_t \left(\eta^c ps^c_{e,t} - \frac{ps^d_{e,t}}{\eta^d} \right), \forall t \in \mathscr{T}_s \backslash \left\{ \underline{t}_s \right\} \tag{22}$$

$$ps_{e,t} = ps^c_{e,t} - ps^d_{e,t} \tag{23}$$

$$SOC^{min}_e \leq soc_{e,t} \leq SOC^{max}_e \tag{24}$$

$$0 \leq ps^c_{e,t} \leq PS^c_{e,t} \tag{25}$$

$$0 \leq ps^d_{e,t} \leq PS^d_{e,t} \tag{26}$$

The state transition function $T_s(x_s, u_s, \omega_s)$ is given by the energy balance equation Eq. 22 when $t = \overline{t}_s$. The energy balance for other values of t and the remaining constraints Eq. 23, 24, 25 and 26 are in the set of admissible controls $U_s(x_s, \omega_s)$.

2.4.3. Objective

A common OPF objective is minimizing the operating costs accounting for the constraints and losses in the grid. Recall that under perfect competition, the solution of global cost minimization equals profit maximization for each individual unit, and the dual values of the bus power balance from the OPF solution, also known as LMP, represents the electricity price for that bus. The objective in this case is to minimize the sum of generator operating costs and load shedding costs. The costs are given by constant marginal costs and must be summed for all generators and loads at all buses for all time steps as shown in Eq. 27, and define the stage-objective $C_s(x_s, u_s, \omega_s)$ in the SDP formulation in Eq. 2.

$$C_s(x_s, u_s, \omega_s) = \sum_{b \in \mathscr{B}} \sum_{t \in \mathscr{T}_s} \left(\sum_{g \in \mathscr{G}_b} C_g \, p_{g,t} + \sum_{d \in \mathscr{D}_b} C_d \, pls_{d,t} \right) \Delta T_t \tag{27}$$

2.5. Noise

This paper will study the effect of uncertainty from solar PV generation in combination with energy storage. Demand uncertainty will have similar implication on the result, but this has not been analyzed.

2.5.1. Solar PV forecasting

Solar PV forecasting can be grouped into statistical and physical methods, or a combination of these. The statistical methods exploit the properties of historical data, while the physical methods include Numerical Weather Prediction (NWP), sky imagery and satellite imaging. The forecasting technique for solar PV generation is highly dependent on forecasting horizon. Statistical methods are commonly used for short-term forecasts up to six hours, while NWP is used for forecasts up to 15 days ahead [43].

The maximum generation from solar PV depends on the PV panel's size, geographical location, direction and angle, and the time of day and year. Weather type also has a significant impact on the generation, and is commonly classified into different categories, such as *clear sky, partly clouded* and *overcast*. The weather type influences both the total daily generation as well as the generation variability [44]. A sunny day will, for example, provide stable high generation with low uncertainty, while the generation will fluctuate rapidly on partly clouded days due to the rapid changes in cloud cover.

The CI is the ratio between actual generation and the theoretical maximum at that time and location Eq. 28. The CI value is between 0 and 1 and quantifies how much the solar radiation passes through the clouds. It is commonly used for statistical analysis of the solar PV generation.

$$\phi_{r,s} = \frac{p_{r,t}}{P_{r,t}^{max}} \tag{28}$$

A probabilistic model for the CI will be used in this paper, where the expected value and variance are assumed to be known ahead. The CI is always between 0 and 1, which also applies for the beta distribution that is commonly used for solar PV CI [45–47]. The CI $\Phi_{r,s}$ is undefined for the hours where the theoretical maximum generation is zero due to zero division, but the resulting generation will of course be zero.

2.5.2. Beta distribution

The probability density function (PDF) of the beta distribution on standard form is shown in Eq. 29 where $B(1; \alpha, \beta)$ is a distribution specific constant given by the beta function Eq. 31 that ensures the distribution sums up to one. The cumulative distribution function is shown in Eq. 30.

$$f(x; \alpha, \beta) = \frac{1}{B(1; \alpha, \beta)} x^{\alpha-1} (1-x)^{\beta-1} \tag{29}$$

$$F(x; \alpha, \beta) = \frac{B(x; \alpha, \beta)}{B(1; \alpha, \beta)} \tag{30}$$

$$B(\alpha, \beta) = \int_0^x t^{\alpha-1} (1-t)^{\beta-1} dt \quad \alpha, \beta \geq 0, \ 0 \leq x \leq 1 \tag{31}$$

For a known expected value μ and variance σ^2, the beta distribution coefficients can be found from Eq. 32 and 33 [48].

$$\alpha = \frac{\mu^2(1-\mu)}{\sigma^2} - \mu \tag{32}$$

$$\beta = \left(\frac{\mu(1-\mu)}{\sigma^2} - 1 \right)(1-\mu) \tag{33}$$

2.5.3. Uncertainty sampling

The noise in SDP must be stage-wise independent. However, dependencies in noise across stages can be respected by modelling the noise with state variables, but will also increase the dimensionality of

the optimization problem and thus have not been accounted for in this paper.

The true continuous probability distribution must be represented with a discrete probability distribution with M discrete points ϕ_m and their corresponding probability ρ_m, where the probabilities sums up to one Eq. 34. By selecting initial probabilities $\hat{\rho}_m$, the corresponding boundary values $\delta_1, \cdots, \delta_{M-1}$ where $0 = \delta_0 < \delta_1 < \cdots < \delta_{M-1} < \delta_M = 1$ can be found numerically from Eq. 35. Let $\hat{\phi}_m$ represent an initial solution given by the expected value in the corresponding interval $[\delta_{m-1}, \delta_m]$ as shown in Eq. 36.

$$\sum_{m \in \mathcal{M}} \rho_m = 1 \tag{34}$$

$$\rho_m = \int_{\delta_{m-1}}^{\delta_m} f(\phi) \, d\phi, \ m \in \mathcal{M} \tag{35}$$

$$\hat{\phi}_m = \frac{\int_{\delta_{m-1}}^{\delta_m} \phi f(\phi) \, d\phi}{\int_{\delta_{m-1}}^{\delta_m} f(\phi) \, d\phi}, \ m \in \mathcal{M} \tag{36}$$

The discrete distribution given by $\hat{\rho}_m, \hat{\phi}_m$ will give the same expected value as the true distribution, but the variance will be lower. Let ρ_m, ϕ_m represent the improved discrete distribution for the boundary values δ_m. The improved discrete distribution can be found by minimizing the squared difference between the initial distribution points $\hat{\phi}_m$ and ϕ_m, constrained such that expected value and variance from continuous distribution are conserved [49].

$$
\begin{aligned}
\min_{\rho, \phi} \quad & \sum_{m \in \mathcal{M}} \rho_m \left(\phi_m - \hat{\phi}_m \right)^2 \\
\text{subject to} \quad & \sum_{m \in \mathcal{M}} \rho_m = 1 \\
& \sum_{m \in \mathcal{M}} \rho_m \phi_m = \mu \\
& \sum_{m \in \mathcal{M}} \rho_m \phi_m^2 = \mu^2 + \sigma^2
\end{aligned}
\tag{37}
$$

2.6. Simulation

A multi-stage stochastic optimization model provides a strategy for how to optimally operate at a given stage and state for a given realization of the noise. A simulation of multiple scenarios can give a probabilistic LMP and SMV. The scenarios are sampled from the noise distribution(s) and optimized with the stage-wise MP-OPF models beginning at the first stage and using the final state for each stage as the initial state for the next state. This procedure is similar to the one described in Fosso et al. [23] and is shown in Algorithm 1.

2.7. Model summary

The SDP optimization procedure is illustrated in Fig. 4, where stages are shown at the x-axis and the discrete states at the y-axis. Each stage-wise problem s is solved for each discrete state n and each scenario m, and a SEV-function is approximated using the expected gradients $\lambda_{s,n}$ for each discrete state n. The stage-wise problems are repeated extensively in Appendix A. Algorithm 2 summarizes the optimization procedure where ϵ is a convergence threshold.

3. Implementation and numerical values

This section presents implementation details, system topology and the numerical data that will be used to demonstrate the optimal operation and the corresponding prices in a power system with uncertain variable renewable generation and energy storage.

The optimization problem is implemented in the programming language Julia (1.4) using the JuMP modelling language (0.21.3) [50] with the non-linear solver Ipopt (0.6.2) [51]. The power flow equations have

Initialize x_1
for $s \in \mathcal{S}$ **do**
    Sample scenario $\omega_s \in \Omega_s$
    Solve (2) and (5)
    Save LMP (dual value of (18))
    Save SMV (dual value of (23))
    Save EES SOC ($soc_{e,t}$ from (23))
    Initialize incoming state for the next stage with outgo-
    ing state of current stage: $x_{s+1} \leftarrow x'_s$
end for

Algorithm 1. Simulation algorithm.
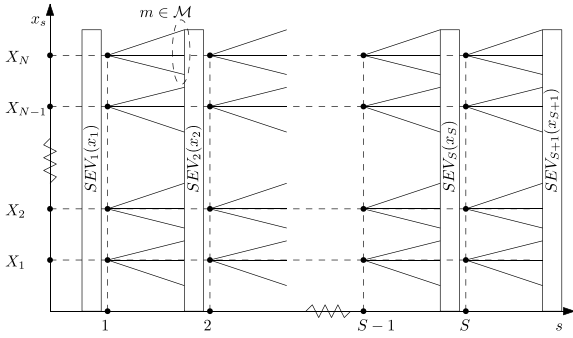
Fig. 4. Stochastic dynamic programming solution procedure.

been implemented using PowerModels (0.17.1) [52] with the multi-period description from [53].

3.1. System topology

Fig. 1 shows the system topology, where bus 1 has an expensive peak generator, bus 2 industrial loads and VRE generation in terms of solar PV, bus 3 has residential loads and battery storage, and bus 4 has a cheaper base generator. The base generator typically represents combined cycle gas turbines (CCGT), where the investment cost is high, and the marginal operating cost is low. The peak generator typically represents open cycle gas turbines (OCGT) where the investment cost is lower and the marginal operating cost is higher. The base generator demands a relatively higher duration compared to the peak generator in order to be profitable. Thermal plants also have limitations in start-up time,

ramping rates, minimum generation limits and marginal operating cost varying with generation [54], which have not been modelled in this paper. Section 3.6 presents the combination of generation capacities that will be analyzed in Section 4.

3.2. Time steps and stages

The time step length in the MP-OPF problems is one hour, and there are three time steps between each stage. That means perfect foresight three hours ahead at a stage, and that the uncertainty in the next stage is revealed every three hours. The planned operation will also be adjusted every three hours.

3.3. Solar PV clearness index

The CI expected value and variance are assumed to be known ahead based on forecasts. Three different weather types are used: sunny, partly clouded and overcast. Both the continuous and discrete probability distributions are shown in Fig. 5 as well as the expected value and standard deviation, and assumes a similar pattern as described in [44]. The discrete probability distribution has been obtained using the method described in Section 2.5.3 with probability intervals 5%, 20%, 50%, 20% and 5%. Table 1 shows the sequence of weather types for the respective days used in the simulations. The probability distribution and the maximum PV generation are shown in Fig. 6.

The SDP algorithm does not propose a single solution to the problem, but an operation strategy for all state combinations at any time. To verify the strategy, different scenarios are sampled using the continuous probability distribution, and simulated based on the SDP strategy.

For real-time operation, the ideal solution is to update the CI forecast, and the corresponding operation strategy as often as possible. It is

Initialize $SEV_{S+1}(x_{S+1})$
repeat
    for $s \in reverse(\mathcal{S})$ **do**
        for $n \in \mathcal{N}$ **do**
            for $\omega_s \in \Omega_s$ **do**
                Solve (2) and (5) for $x_s = X_n$ and ω_s
            end for
            Find $\lambda_{s,n}$(6)
        end for
        Approximate $SEV_s(x)$, equation (7) to (10)
    end for
    $SEV_{S+1}(x) \leftarrow SEV_1(x)$
until Terminate when final end value function has con-
verged: $\left| SEV_{S+1}(X_n) - SEV_1(X_n) \right| < \epsilon, \ \forall \ n \in \mathcal{N}$
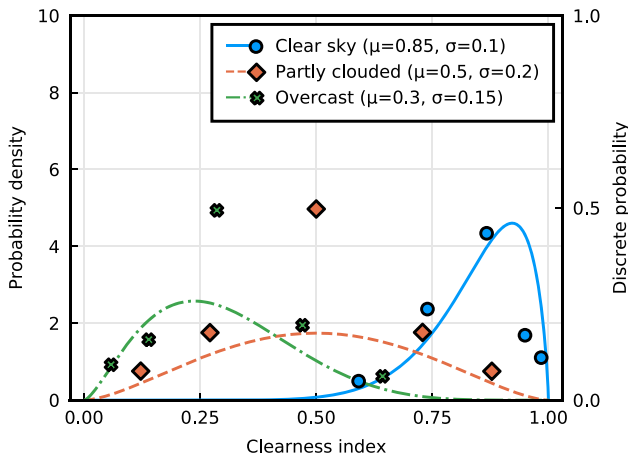
Algorithm 2. SDP algorithm.

Fig. 5. Continuous and discrete probability distributions of clearness index for different weather types with 5 samples per distribution.

Table 1
Expected value and standard deviation of clearness index beta distribution for the simulated days.

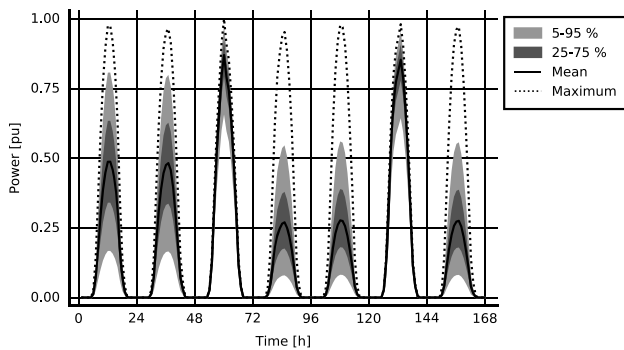| Day	Weather type
1	Partly clouded
2	Partly clouded
3	Sunny
4	Overcast
5	Overcast
6	Sunny
7	Overcast

Fig. 6. Solar PV one week probabilistic profile.

also possible to use a combination of different forecasting techniques to cover the different time horizons as accurately as possible. In this paper, the prices and operation are only studied from one point in time.

3.4. Load forecast time series

The system load is typically subject to uncertainty, often represented as a Gaussian distribution. There is also often a correlation between load and VRE generation since they both depend on weather. Neither the load uncertainty nor the correlation between load and generation are not modelled in this paper such that the impact of generation uncertainty is clearer. The system has two loads, as shown in Fig. 1, an industrial and a residential load where the profiles for the loads are shown in Fig. 7, where the profiles have been generated using the FASIT model developed by SINTEF Energy Research [55]. Note that the weekday profiles
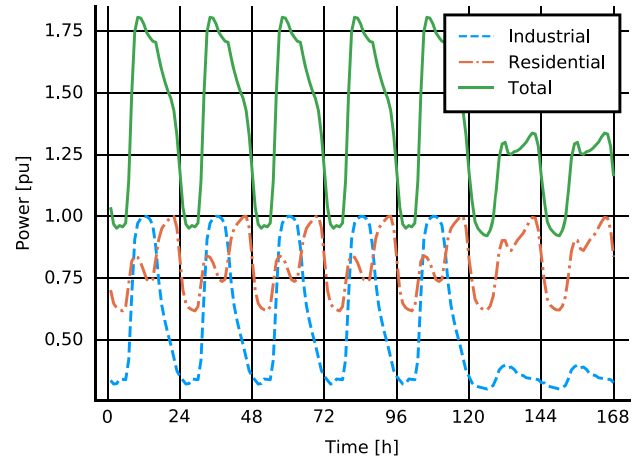

Fig. 7. Industrial and residential weekly load profile.

differ from the weekends. The time series shows the one week profile.

3.5. Generation and storage capacities and cost

The base generator has a marginal operating cost of 20 € /MWh and the peak generator 30 € /MWh, and start and stop costs are neglected. The solar PV generation and storage have zero marginal cost. The scarcity price in the system is 100 € /MWh for both loads. The storage duration is 4 hours, meaning that it takes 4 hours to empty a full battery at maximum discharge. The storage efficiency is 95% for both charging and discharging. The maximum charge and discharge power are equal.

3.6. Test cases

The price making will be studied for four different cases with different combinations of generation and storage capacities as shown in Table 2. The first case includes only thermal generation to illustrate how the price is set by the marginal unit at the respective nodes. Moreover, the next case will show how the introduction of solar PV and storage will change the price. Finally, the last case will show a system with no thermal generation to set the price. The transmission capacity between bus 2 and 3 is limited in all cases, but the maximum capacity is increased when introducing VRE.

4. Results

This section presents the numerical results of the cases outlined in Section 3. Both optimal dispatch, LMP and SMV based on the resulting marginal values will be studied.

For the examples involving stochastic solar PV generation and energy storage, the SMV is presented as a function of time and state of charge. The interpretation of the SMV will also be discussed. Optimal generation and storage operation, and energy prices are presented as percentiles based on multiple simulations using the continuous distribution of the uncertain variable.

Table 2
Test case generation, EES and transmission capacities.

| Case name	Base	Peak	PV	Storage	Line 2-3 limit
Only thermal (Section 4.1)	1.5	0.5	0.0	0.0	0.7
Thermal & PV (Section 4.2)	1.5	0.5	4.0	0.0	0.7
Thermal, PV & EES (Section 4.3)	1.0	1.0	4.0	0.8	0.8
PV & EES (Section 4.4)	0.0	0.0	9.5	10.0	5.0

4.1. Only thermal generation

In a system with only thermal power generation and fixed demand, the price is set by the marginal producing unit if the capacity is higher than the load. For a congested grid, the price will also vary between the different nodes, as illustrated in this simple 4-bus system with two thermal generators and two loads.

Fig. 8a shows the two system loads and generators over the first 24 hours, and Fig. 8b shows the corresponding LMPs. The price is 20 € /MWh when the base generator can meet the entire load, and 30 € /MWh when the peak generator also must contribute. From hour 12, the LMPs are different between the nodes since the transmission line between bus 2 and 3 has reached its limit, hence the peak generation must replace some of the base generation to prevent overloading of the line. In this situation, the base generator will be the marginal unit for the residential load since it is not able to generate at maximum capacity so the two nodes get different prices.

4.2. Variable renewable generation

As explained earlier, introduction of variable renewable generation with zero marginal cost will reduce the prices when the existing generation capacities are unchanged due to the merit order effect. Solar PV generation is installed at bus 2.

The resulting generation and price are shown in Fig. 9a and b respectively. Note that the base generator gets a high ramp rate due to the high solar PV generation in the middle of the day, and the shape of the curve is often referred to as the "duck curve" [56]. The solar PV generation makes the peak generation redundant and reduces the price at both buses compared to the previous case. At the middle of the day, the transmission capacity between node 2 and 3 is insufficient to meet the demand with solar PV generation, thus the price is set by the base generator for the residential load. However, the industrial load can meet all its demand with solar PV generation that becomes the marginal generation unit at this bus, thus the price becomes zero.

(a) Load and generation.

(b) System LMP.

Fig. 8. Simulation of case with only thermal generation.
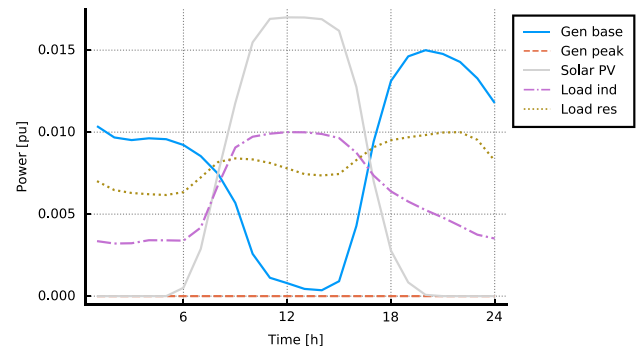
(a) Load and generation.
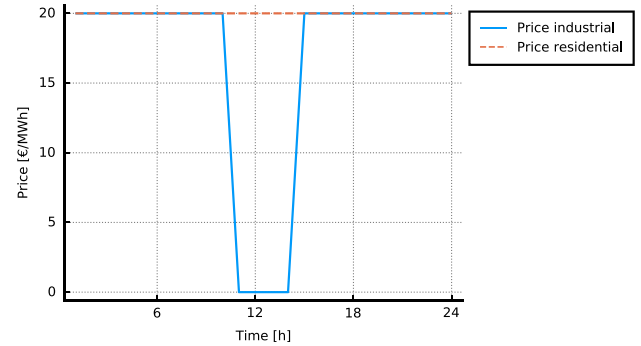
(b) System LMP.

Fig. 9. Simulation of case with thermal and solar PV generation.
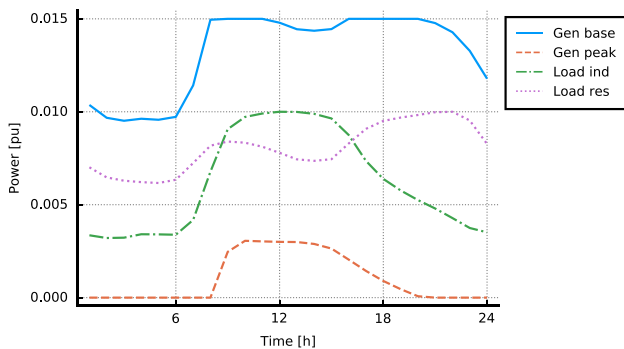
4.3. Energy storage

In the previous cases, the optimal generation and energy price were only dependent on the present load and PV generation. When energy storage is introduced, the optimal strategy and the corresponding energy price also depend on the state of charge of the energy storage. Moreover, the state depends on previous decisions, which in turn are influenced by uncertainty. The stochastic result will therefore be studied for this case and the following cases.

In a competitive market, the VRE will typically displace some of the base generation that depends on a high duration to recover its costs. Some of the base capacity has therefore been replaced with peak capacity in the case setup.
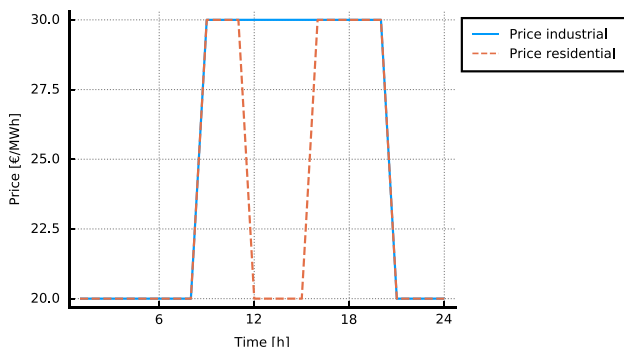
Fig. 10a shows the SMV as a function of time and storage SOC. As emphasized earlier, the SMV represents the marginal future value by storing an additional unit of energy. The SMV has several interesting interpretations. Under perfect competition, the individual energy storage profit is maximized by bidding the SMV, and the solution of individual profit maximization for all units equals the system optimal solution. The SMV will therefore set the LMP when the storage is the marginal unit at that node. Since the marginal value has been found using SDP, it also captures uncertainty, hence the value represents a weighted probability of the prices of the units in the system at any time and SOC taking into account the probabilistic forecast of PV.

The optimal usage of the storage in this case involves charging from the cheap generators such that the storage can discharge later in order to avoid using the expensive generators or load shedding.

The SMV is close to zero for maximum SOC around mid-day all the days (hours 12, 36 and 60). This occurs when the solar PV generation is high, and it is likely that the battery can be charged to maximum before the solar PV generation reduces. It also indicates that the energy from the EES should be used rather than the thermal generation since the SMV is less than the marginal cost of both thermal units. The SMV is higher in the evening (hours 18, 42 and 66), when there is no or very low solar PV generation and a relatively high load. For very low SOC, the SMV is close

(a) Storage marginal value.

(b) Storage state-of-charge.

(c) LMP at industrial bus.
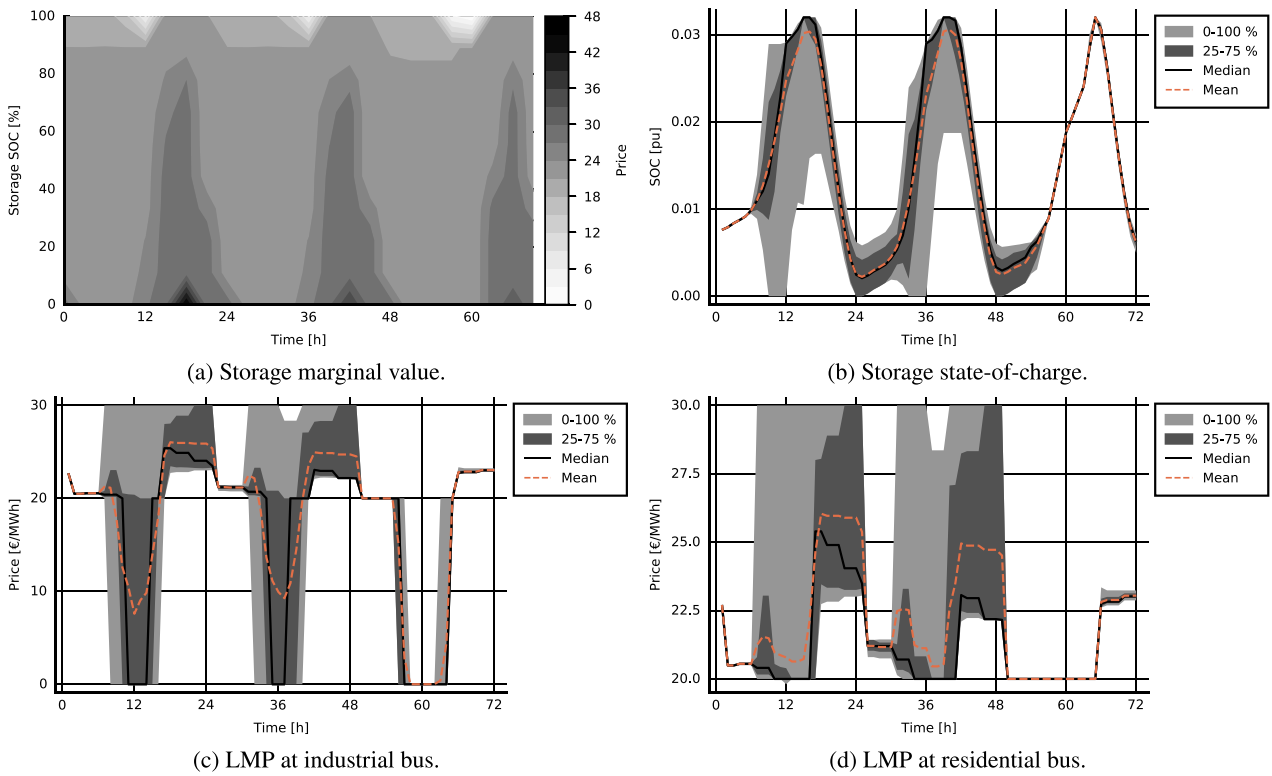

(d) LMP at residential bus.

Fig. 10. Multiple simulations of case with thermal and solar PV generation and energy storage.

to 50 and higher than the marginal cost of both thermal generators. This indicates that the thermal generators should be used rather than the EES unless the thermal generators are insufficient to prevent load shedding. The scarcity price is 100 € /MWh, and a SMV at 50 indicates a significant probability of scarcity price in this situation. Finally, observe that the SMV is between 20 and 30 in most situations. That is when the EES is used to balance the probability of being able to meet the demand with base generation versus peak generation for the different combinations of time and SOC taking into account the probabilistic forecast of PV.

Fig. 10c and d show the price percentiles for 50 simulations sampled from the continuous probability distribution of the solar PV generation at the bus with industrial loads and residential loads respectively. The price will often be zero at the industrial node around mid-day as the storage does not have capacity to store the surplus generation. At the same time, the residential node will not get zero price as the transmission capacity between the nodes is at the maximum limit. Uncertainty plays an important role in the price making for the system as the spread for both nodes is quite significant.

The resulting SOC in Fig. 10b shows that almost the entire storage capacity is utilized to minimize the generation costs.

4.4. Only renewable generation and energy storage

In the final case, the thermal units are removed completely, and the solar PV generation and EES capacity are sized up considerably. The EES must be large enough to meet all the demand through the evening and night when the solar PV is not generating. Moreover, the solar PV must be sized such that it provides enough generation for both the current demand as well as the evening/night demand - even for a day with relatively low generation. An important assumption to avoid imperfect competition is that the EES actually represents multiple aggregated EES with different operators. Otherwise, the EES operator could maximize its profit by bidding the scarcity price.

The price will now be set solely by the scarcity price, and future foresight is even more important for the electricity price. The

optimization model is therefore using a one-week generation forecast.

Fig. 11a shows the SMV for all states and the corresponding expected solar PV generations are shown in Fig. 6. As observed earlier, the SMV follows the pattern from the solar PV generation. High generation reduces the marginal value of stored energy and vice versa. Another interesting observation is that due to expected low generation from hour 72, the marginal value of the storage increases upfront, indicating it is important to increase the SOC before entering the days with expected low generation. Likewise, the SMV decreases towards hour 120 as the expected generation the next day is high.

The corresponding LMPs are shown in Fig. 11c and d. The price is on average low until the end of day 3 (around hour 66), where the SOC has been built up to meet the expected low generation the next two days. However, the spread in price is high due to the high variability in generation. Then the price increases instantaneously and the further development has a high spread and high expected value. Finally, the price reduces at the end as the expected further generation is equal to the generation in the beginning.

Note that the price change is no longer dominated by the solar PV generation pattern as in previous cases, but rather the future probability of scarcity. This market price will be attractive for suppliers of flexibility capable of shifting energy over several days by utilizing the price variations. They will also get paid for reducing the risk of scarcity rather than getting paid only if scarcity occurs.

The differences between the LMP for the industrial and residential nodes occur when some of the solar PV generation is curtailed due to insufficient load and transmission capacity. The development in SOC in Fig. 11b clearly shows how the SOC is built up ahead of the period with low generation and emptied towards the period with high generation.

5. Discussion

VRE and EES play a key role in the future fully renewable energy system, and they will also have significant implications on the market equilibrium and electricity prices. As already emphasized in previous
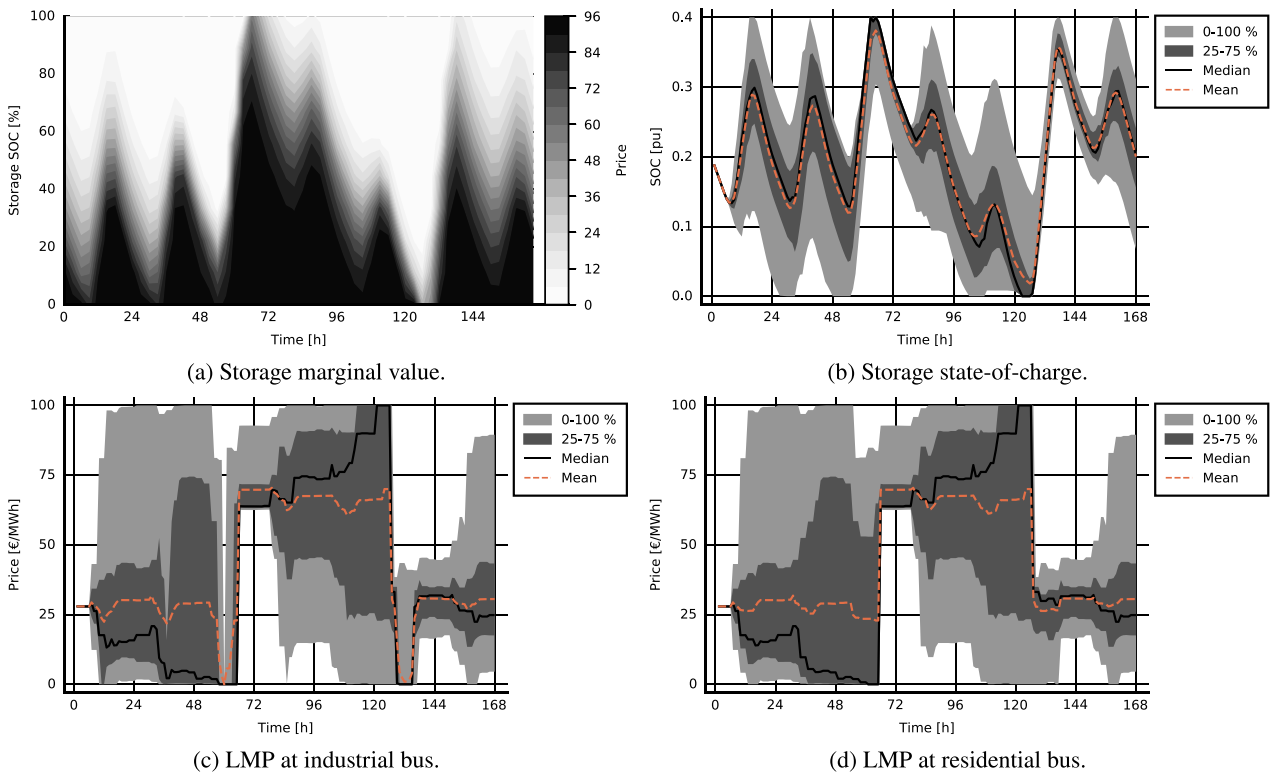
(a) Storage marginal value.

(b) Storage state-of-charge.

(c) LMP at industrial bus.

(d) LMP at residential bus.

Fig. 11. Multiple simulations of case with only solar PV generation and EES.

literature, the short-term consequence of increasing VRE generation is a reduction in electricity price due to the merit order effect as shown in Section, but also increased volatility. However, the price volatility can be reduced by EES. When uncertainty is accounted for, the combination of VRE and EES will result in a probabilistic price spanning between the price of the most and the least expensive unit.

While previous studies primarily focus on the electricity price in systems combining VRE with thermal generation, this paper also focuses on the price formation when most of the generation is supplied by VRE sources. If EES replaces some of the dispatchable capacity such that the system depends on EES to meet peak demand, scarcity may occur and load shedding can be considered as the most expensive unit. The electricity price can then be seen as an arbitrage against the risk of scarcity. An interesting consequence of this is that the scarcity price becomes effective without scarcity necessarily occurring, and the price can be seen as a precaution against scarcity.

The weighted scarcity price creates possibilities for flexible loads with marginal price below the scarcity price to enter the market. A flexible load can in its simplest form be modelled as a dispatchable negative generator, meaning that the load can be curtailed at a predetermined cost with no need of delivering the lost load at a later stage. A flexible load can also represent shifting of load, and can be modelled as an EES where a penalty applies when deviating from the ideal SOC.

Flexible loads will in general contribute to reducing the high prices by reducing the risk of scarcity. The scarcity price has a practical implication although the electricity price rarely reaches the full scarcity price. With sufficient flexibility in the system to fully eliminate the risk of scarcity, the maximum price will be set by the most costly flexible unit. Likewise, the flexible loads will also increase the low prices by reducing the risk of generation curtailment.

5.1. Future work

Possible steps towards a more practical applicable model could involve modelling of flexible demand, and also other uncertainties such

as demand and generation from wind. Uncertainties are often correlated, with both auto-correlation and correlation between uncertainties. Both handling correlated uncertainty and additional EES will require new state variables, which scale poorly with SDP although the scalability can be improved using splines [27]. A more common method for handling increasing number of state variables is using Stochastic Dual Dynamic Programming (SDDP) [57], where the model formulation must be convex. The infinite horizon method suggested in this paper is not feasible to implement in SDDP, but cyclic graphs and discount factors provides an interesting alternative to infinite horizon optimization in SDDP [31].

Multi-stage stochastic models are in general computationally intensive to solve, and scalability often goes hand in hand with convexity and linearity such as for SDDP. Real-life power systems are neither linear nor convex. Thermal generators as well as hydro power plants have discontinuous production functions due to rigorous minimum generation limits, and the power flow equations are both non-linear and non-convex. Convexification and linearization must therefore be performed cautiously since the result could easily deviate from the true optimal solution. However, recent research has proposed methods to handle integer variables in the SDDP framework [58].

In a competitive market where each individual unit seeks to maximize its profit and where the price is given exogenously, it is important to also recall that the price is set by the VRE generation and demand. Additionally, there will be a strong correlation between the generation and demand uncertainty, and the price uncertainty. Managing uncertainty in price yields a non-linear optimization problem that can be handled in several ways [59,60].

EES is subject to degradation caused by its operational pattern, and Aaslid et al. [32] indicate that EES degradation could be an important factor in combination with generation uncertainty.

The proposed model will also provide storage end value functions for all stages. The end value function can be used as boundary conditions for a more detailed finite horizon storage model [61]. This principle has been described for hydro power in [62] and combines detailed storage

modelling and stochastic modelling with long foresight while still keeping the computational burden modest.

Flexibility has traditionally been provided by centralized generation units, but has to a greater extent been decentralized through flexible demand. A preferred approach is to solve operational challenges in the electricity system as close as possible to their origin. Until now, power markets have been driven by development and limitations on transmission level. However, solving problems locally demands local price signals reflecting the local challenges. A good starting point for this is to study the LMP in these systems as it can give valuable insight into how to design and operate future electricity systems with more distributed resources.

6. Conclusions

The road towards a zero emission electricity system calls for massive integration of VRE and flexibility to ensure a secure and efficient supply. These major changes will influence the price-making process in competitive markets. While capacity inadequacy is the main driver for high prices in markets dominated by thermal generation, energy inadequacy is the main driver for high price in markets dominated by VRE and EES. Managing uncertainty is crucial to balance optimal operation by reducing generation curtailment while keeping the risk of scarcity sufficient low.

This paper presents a multi-stage stochastic electricity market model including grid constraints, EES and VRE. The model uses SDP to solve a multi-stage MP-OPF problem under uncertain VRE generation, EES and administrative scarcity pricing, both with and without dispatchable generation. The stage-wise problems are interconnected with SEV functions describing the marginal value of stored energy both in time

and with respect to SOC represented as cubic spline functions. The results shows how the LMP can be seen as an arbitrage between the marginal cost of the units in the system, where load shedding is the most expensive unit through the scarcity price. The SMV depends on the state of all EES in the system as well as expected future VRE generation and can be used to determine the optimal operation of EES, and will set the price when EES is the marginal generating unit.

CRediT authorship contribution statement

Per Aaslid: Conceptualization, Methodology, Software, Formal analysis, Investigation, Visualization, Writing - original draft. **Magnus Korpås:** Conceptualization, Writing - review & editing. **Michael M Belsnes:** Writing - review & editing, Project administration. **Olav B Fosso:** Writing - review & editing, Supervision.

Declaration of Competing Interest

The authors declare that they have no known competing financial interests or personal relationships that could have appeared to influence the work reported in this paper.

Acknowledgements

Appendix A. Summary of optimization problem

A1. Stage-wise optimization problem

$$
\begin{aligned}
\min_{u_s}\{C_s(x_s, u_s, \omega_s) &- sev_{s+1}\} \\
\text{s.t. } x_s' &= T_s(x_s, u_s, \omega_s) \\
sev_{s+1} &\leq SEV_{s+1}\left(x_s'\right) \\
u_s &\in U_s(x_s, \omega_s)
\end{aligned}
$$

A2. State variables

Incoming state is given by the initial SOC and outgoing state by the end SOC of the stage-wise problem.

$$
\begin{aligned}
x_s &= \left\{soc_{e,\underline{t}_s}\right\} \\
x_s' &= \left\{soc_{e,\bar{t}_s}\right\} \\
&\qquad \forall e \in \mathscr{E}_b, b \in \mathscr{B}
\end{aligned}
$$

A3. Control variables

All variables except the state variables are considered control variables and are set either explicit or implicit.

$$
u_s = \left\{p_{b,t}, p_{g,t}, p_{r,t}, p_{e,t}, ps_{e,t}^c, ps_{e,t}^d, p_{d,t}, pls_{d,t}, soc_{e,\tilde{t}}, \theta_{b,t}\right\}
$$

$$
\forall b \in \mathscr{B}, g \in \mathscr{G}_b, r \in \mathscr{R}_b, e \in \mathscr{E}_b, d \in \mathscr{D}_b, t \in \mathscr{T}_s, \tilde{t} \in \mathscr{T}_s \backslash \left\{\underline{t}_s, \bar{t}_s\right\}
$$

A4. Noise

$$\omega_s = \{\phi_{r,s}\} \quad \forall r \in \mathscr{R}_b, b \in \mathscr{B}$$

A5. Stage-objective

$$C_s(x_s, u_s, \omega_s) = \sum_{b \in \mathscr{B}} \sum_{t \in \mathscr{T}_s} \left(\sum_{g \in \mathscr{G}_b} C_g \, p_{g,t} + \sum_{d \in \mathscr{D}_b} C_d \, pls_{d,t} \right) \Delta T_t$$

A6. State-transition

The state transition is given by the energy balance for the final time step in current stage. The incoming state x_s is connected implicitly with the outgoing state x_s' through the admissible controls $u_s \in U_s(x_s, \omega_s)$.

$$soc_{e,\bar{t}_s} = soc_{e,\bar{t}_s - 1} + \Delta T_t \left(\eta^c ps_{e,\bar{t}_s}^c - \frac{ps_{e,\bar{t}_s}^d}{\eta^d} \right)$$

A7. Admissible controls

The admissible controls include all constraints except the state transition:

$$U_s(x_s, u_s, \omega_s) = u_s : \begin{cases}
p_{b,t} = \sum_{(i,k) \in \mathscr{L}_b} B_{ik}(\theta_{i,t} - \theta_{k,t}) - P_{ik}^{max} \leq B_{ik}(\theta_{i,t} - \theta_{k,t}) \leq P_{ik}^{max} \\[2mm]
\Theta_b^{min} \leq \theta_{b,t} \leq \Theta_b^{max} \\[2mm]
p_{b,t} = \sum_{g \in \mathscr{G}_b} p_{g,t} + \sum_{r \in \mathscr{R}_b} p_{r,t} - \sum_{e \in \mathscr{E}_b} p_{e,t} - \sum_{d \in \mathscr{D}_b} p_{d,t} \\[2mm]
0 \leq p_{g,t} \leq P_g^{max} \\[2mm]
0 \leq p_{r,t} \leq \phi_{r,s} \cdot P_{r,t}^{max} \\[2mm]
p_{d,t} = PD_{d,t} - pls_{d,t} \geq 0 \\[2mm]
ps_{e,t} = ps_{e,t}^c - ps_{e,t}^d \\[2mm]
SOC_e^{min} \leq soc_{e,t} \leq SOC_e^{max} \\[2mm]
0 \leq ps_{e,t}^c \leq PS_{e,t}^c \\[2mm]
0 \leq ps_{e,t}^d \leq PS_{e,t}^d \\[2mm]
soc_{e,\tilde{t}} = soc_{e,\tilde{t}-1} + \Delta T_{\tilde{t}} \left(\eta^c ps_{e,\tilde{t}}^c - \frac{ps_{e,\tilde{t}}^d}{\eta^d} \right) \\[2mm]
\forall b \in \mathscr{B}, g \in \mathscr{G}_b, r \in \mathscr{R}_b, e \in \mathscr{E}_b, d \in \mathscr{D}_b, t \in \mathscr{T}_s, \tilde{t} \in \mathscr{T}_s \setminus \{\bar{t}_s\}
\end{cases}$$

References

[1] International Renewable Energy Agency, Global energy transformation: a roadmap to 2050 (2019 edition). Technical Report, IRENA, 2019.978-92-9260-121-8

[2] C. Kost, S. Shammugam, V. Jülch, H.-T. Nguyen, T. Schlegl, Levelized cost of electricity renewable energy technologies. Technical Report, Fraunhofer institute for solar energy systems ise, 2018.

[3] F. Sensfuß, M. Ragwitz, M. Genoese, The merit-order effect: a detailed analysis of the price effect of renewable electricity generation on spot market prices in Germany, Energy Policy 36 (8) (2008) 3086–3094, https://doi.org/10.1016/j.enpol.2008.03.035.

[4] J.C. Ketterer, The impact of wind power generation on the electricity price in Germany, Energy Econ. 44 (2014) 270–280, https://doi.org/10.1016/j.eneco.2014.04.003.

[5] S. Djørup, J.Z. Thellufsen, P. Sorknæs, The electricity market in a renewable energy system, Energy 162 (2018) 148–157, https://doi.org/10.1016/j.energy.2018.07.100.

[6] C.K. Woo, J. Moore, B. Schneiderman, T. Ho, A. Olson, L. Alagappan, K. Chawla, N. Toyama, J. Zarnikau, Merit-order effects of renewable energy and price divergence in California's day-ahead and real-time electricity markets, Energy Policy 92 (2016) 299–312, https://doi.org/10.1016/j.enpol.2016.02.023.

[7] D. Azofra, E. Jiménez, E. Martínez, J. Blanco, J.C. Saenz-Díez, Wind power merit-order and feed-in-tariffs effect: A variability analysis of the Spanish electricity market, Energy Conver. Manag. 83 (2014) 19–27, https://doi.org/10.1016/j.enconman.2014.03.057.

[8] J. Cludius, H. Hermann, F.C. Matthes, V. Graichen, The merit order effect of wind and photovoltaic electricity generation in Germany 2008-2016 estimation and distributional implications, Energy Econ. 44 (2014) 302–313, https://doi.org/10.1016/j.eneco.2014.04.020.

[9] L. Hirth, The market value of variable renewables. The effect of solar wind power variability on their relative price, Energy Econ. 38 (2013) 218–236, https://doi.org/10.1016/j.eneco.2013.02.004.

[10] C. Helm, M. Mier, Efficient diffusion of renewable energies: a roller-coaster ride. Technical Report, University of Oldenburg, Department of Economics, 2016.

[11] M. Korpås, A. Botterud, Optimality conditions and cost recovery in electricity markets with variable renewable energy and energy storage, 2020.

[12] R. Green, N.V. Vasilakos, The long-term impact of wind power on electricity prices and generating power, SSRN Electron. J. (2012), https://doi.org/10.2139/ssrn.1851311.

[13] IEA, Energy Storage. Technical Report, International Energy Agency, Paris, 2020.

[14] W. Cole, A. Frazier, Cost projections for utility-scale battery storage: 2020 update. Technical Report, National Renewable Energy Laboratory (NREL), Golden, CO (United States), 2020, https://doi.org/10.2172/1665769.

[15] F. Díaz-González, A. Sumper, O. Gomis-Bellmunt, R. Villáfáfila-Robles, A review of energy storage technologies for wind power applications, Renewable and sustainable energy reviews 16 (4) (2012) 2154–2171, https://doi.org/10.1016/j.rser.2012.01.029.

[16] H. Zhao, Q. Wu, S. Hu, H. Xu, C.N. Rasmussen, Review of energy storage system for wind power integration support, Appl. Energy 137 (2015) 545–553, https://doi.org/10.1016/j.apenergy.2014.04.103.

[17] N. Li, C. Uckun, E.M. Constantinescu, J.R. Birge, K.W. Hedman, A. Botterud, Flexible operation of batteries in power system scheduling with renewable energy, IEEE Trans. Sustain. Energy 7 (2) (2016) 685–696, https://doi.org/10.1109/TSTE.2015.2497470.

[18] M. Arbabzadeh, R. Sioshansi, J.X. Johnson, G.A. Keoleian, The role of energy storage in deep decarbonization of electricity production, Nature Commun. 10 (1) (2019) 1–11, https://doi.org/10.1038/s41467-019-11161-5.

[19] D. Krishnamurthy, C. Uckun, Z. Zhou, P.R. Thimmapuram, A. Botterud, Energy storage arbitrage under day-ahead and real-time price uncertainty, IEEE Trans. Power Syst. 33 (1) (2017) 84–93, https://doi.org/10.1109/tpwrs.2017.2685347.

[20] R. Sioshansi, P. Denholm, T. Jenkin, J. Weiss, Estimating the value of electricity storage in PJM: arbitrage and some welfare effects, Energy Econ. 31 (2) (2009) 269–277, https://doi.org/10.1016/j.eneco.2008.10.005.

[21] K.R. Ward, R. Green, I. Staffell, Getting prices right in structural electricity market models, Energy Policy 129 (2019) 1190–1206, https://doi.org/10.1016/j.enpol.2019.01.077.

[22] S. Stoft, Power system economics: designing markets for electricity, IEEE Press, 2002, https://doi.org/10.1109/MPAE.2003.1180363.

[23] O.B. Fosso, A. Gjelsvik, A. Haugstad, B. Mo, I. Wangensteen, Generation scheduling in a deregulated system. the norwegian case, IEEE Trans. Power Syst. 14 (1) (1999) 75–80, https://doi.org/10.1109/59.744487.

[24] S. Stage, Y. Larsson, Incremental cost of water power, Trans. Am. Inst. Electric. Eng. Part III: Power Apparat. Syst. 80 (3) (1961) 361–364, https://doi.org/10.1109/AIEEPAS.1961.4501045.

[25] O. Wolfgang, A. Haugstad, B. Mo, A. Gjelsvik, I. Wangensteen, G. Doorman, Hydro reservoir handling in Norway before and after deregulation, Energy 34 (10) (2009) 1642–1651, https://doi.org/10.1016/j.energy.2009.07.025.

[26] M.V. Pereira, L.M. Pinto, Stochastic optimization of a multireservoir hydroelectric system: a decomposition approach, Water Resour. Res. 21 (6) (1985) 779–792, https://doi.org/10.1029/WR021i006p00779.

[27] S.A. Johnson, J.R. Stedinger, C.A. Shoemaker, Y. Li, J.A. Tejada-Guibert, Numerical solution of continuous-state dynamic programs using linear and spline interpolation, Oper. Res. 41 (3) (1993) 484–500, https://doi.org/10.1287/opre.41.3.484.

[28] J. Geske, R. Green, Optimal storage, investment and management under uncertainty: it is costly to avoid outages!, Energy J. 41 (2) (2020), https://doi.org/10.5547/01956574.41.2.jges.

[29] R. Bellman, Dynamic Programming, 1, Princeton University Press, 1957.

[30] K.M. Chandy, S.H. Low, U. Topcu, H. Xu, A simple optimal power flow model with energy storage. 49th IEEE Conference on Decision and Control (CDC), IEEE, 2010, pp. 1051–1057, https://doi.org/10.1109/CDC.2010.5718193.

[31] O. Dowson, The policy graph decomposition of multistage stochastic optimization problems, Networks 76 (1) (2020) 3–23, https://doi.org/10.1002/net.21932.

[32] P. Aaslid, M.M. Belsnes, O.B. Fosso, Optimal microgrid operation considering battery degradation using stochastic dual dynamic programming. SEST 2019 - 2nd International Conference on Smart Energy Systems and Technologies, Institute of Electrical and Electronics Engineers (IEEE), 2019, pp. 1–6, https://doi.org/10.1109/SEST.2019.8849150.

[33] A. Papavasiliou, Y. Mou, L. Cambier, D. Scieur, Application of stochastic dual dynamic programming to the real-time dispatch of storage under renewable supply uncertainty, IEEE Trans. Sustain. Energy 9 (2) (2018) 547–558, https://doi.org/10.1109/TSTE.2017.2748463.

[34] P. Girardeau, V. Leclere, A.B. Philpott, On the convergence of decomposition methods for multistage stochastic convex programs, Math. Oper. Res. 40 (1) (2015) 130–145, https://doi.org/10.1287/moor.2014.0664.

[35] A. Gabash, P. Li, Active-reactive optimal power flow in distribution networks with embedded generation and battery storage, IEEE Trans. Power Syst. 27 (4) (2012) 2026–2035, https://doi.org/10.1109/TPWRS.2012.2187315.

[36] G. Carpinelli, G. Celli, S. Mocci, F. Mottola, F. Pilo, D. Proto, Optimal integration of distributed energy storage devices in smart grids, IEEE Trans. Smart Grid 4 (2) (2013) 985–995, https://doi.org/10.1109/TSG.2012.2231100.

[37] D. Kourounis, A. Fuchs, O. Schenk, Toward the next generation of Multiperiod optimal power flow solvers, IEEE Trans. Power Syst. 33 (4) (2018) 4005–4014, https://doi.org/10.1109/TPWRS.2017.2789187.

[38] M.E. Baran, F.F. Wu, Optimal sizing of capacitors placed on a radial distribution system, IEEE Trans. Power Del. 4 (1) (1989) 735–743, https://doi.org/10.1109/61.19266.

[39] M.E. Baran, F.F. Wu, Optimal capacitor placement on radial distribution systems, IEEE Trans. Power Del. 4 (1) (1989) 725–734, https://doi.org/10.1109/61.19265.

[40] D.K. Molzahn, I.A. Hiskens, A survey of relaxations and approximations of the power flow equations, Now Publishers, 2019.

[41] J. Carpentier, Contribution á létude du dispatching économique, Bulletin de la Société Française des Électriciens 3 (8) (1962) 431–447.

[42] B. Stott, J. Jardim, O. Alsaç, DC power flow revisited, IEEE Trans. Power Syst. 24 (3) (2009) 1290–1300, https://doi.org/10.1109/TPWRS.2009.2021235.

[43] M.N. Akhter, S. Mekhilef, H. Mokhlis, N.M. Shah, Review on forecasting of photovoltaic power generation based on machine learning and metaheuristic techniques, IET Renewable Power Generation 13 (7) (2019) 1009–1023, https://doi.org/10.1049/iet-rpg.2018.5649.

[44] S. Alimohammadi, D. He, Multi-stage algorithm for uncertainty analysis of solar power forecasting. IEEE Power and Energy Society General Meeting 2016-Novem, IEEE Computer Society, 2016, pp. 1–5, https://doi.org/10.1109/PESGM.2016.7741199.

[45] A.R. Jordehi, How to deal with uncertainties in electric power systems? A review, Renewable and sustainable energy reviews 96 (2018) 145–155, https://doi.org/10.1016/j.rser.2018.07.056.

[46] A. Soroudi, M. Aien, M. Ehsan, A probabilistic modeling of photo voltaic modules and wind power generation impact on distribution networks, IEEE Syst. J. 6 (2) (2012) 254–259, https://doi.org/10.1109/JSYST.2011.2162994.

[47] Y.M. Atwa, E.F. El-Saadany, M.M. Salama, R. Seethapathy, Optimal renewable resources mix for distribution system energy loss minimization, IEEE Trans. Power Syst. 25 (1) (2010) 360–370, https://doi.org/10.1109/TPWRS.2009.2030276.

[48] N.L. Johnson, S. Kotz, N. Balakrishnan, Continuous Univariate Distributions, 2nd, Wiley & Sons, 1994.

[49] Z. Drezner, D. Zerom, A simple and effective discretization of a continuous random variable, Commun. Stat. - Simulat. Comput. 45 (10) (2016) 3798–3810, https://doi.org/10.1080/03610918.2015.1071389.

[50] I. Dunning, J. Huchette, M. Lubin, JuMP: a modeling language for mathematical optimization, SIAM Rev. 59 (2) (2017) 295–320, https://doi.org/10.1137/15M1020575.

[51] L.T. Wächter Andreas;Biegler, On the implementation of an interior-point filter line-search algorithm for large-scale nonlinear programming, Math. Program. 106 (1) (2006) 25–57, https://doi.org/10.1007/s10107-004-0559-y.

[52] C. Coffrin, R. Bent, K. Sundar, Y. Ng, M. Lubin, PowerModels.jl: an Open-source framework for exploring power flow formulations. 20th Power Systems Computation Conference, PSCC 2018, Institute of Electrical and Electronics Engineers Inc., 2018, pp. 1–8, https://doi.org/10.23919/PSCC.2018.8442948.

[53] F. Geth, C. Coffrin, D.M. Fobes, A flexible storage model for power network optimization, e-Energy 2020 - Proceedings of the 11th ACM International Conference on Future Energy Systems (2020) 503–508.

[54] M.K. Mohammed, O.I. Awad, M.M. Rahman, G. Najafi, F. Basrawi, Abd Alla, R. Mamat, The optimum performance of the combined cycle power plant: A comprehensive review, Renewable and Sustainable Energy Reviews 79 (2017) 459–474, https://doi.org/10.1016/j.rser.2017.05.060.

[55] A.O. Eggen, H. Vefsenmo, FASIT kravspesifikasjon - Versjon 2019. Technical Report, SINTEF Energy Research, 2018.

[56] P. Denholm, M. O'Connell, G. Brinkman, J. Jorgenson, Overgeneration from Solar Energy in California. A Field Guide to the Duck Chart. Technical Report, National Renewable Energy Laboratory (NREL), Golden, CO (United States), 2015, https://doi.org/10.2172/1226167.

[57] M.V.F. Pereira, L.M.V.G. Pinto, Multi-stage stochastic optimization applied to energy planning, Math. Program. 52 (1-3) (1991) 359–375, https://doi.org/10.1007/BF01582895.

[58] J. Zou, S. Ahmed, X.A. Sun, Stochastic dual dynamic integer programming, Math. Program. (2018) 1–42, https://doi.org/10.1007/s10107-018-1249-5.

[59] A. Gjelsvik, M.M. Belsnes, A. Haugstad, An algorithm for stochastic medium-term hydrothermal scheduling under spot price uncertainty. Proc. 13th Power System Computation Conference, Trondheim, Norway, 1999, pp. 1079–1085.

[60] A. Downward, O. Dowson, R. Baucke, Stochastic dual dynamic programming with stagewise dependent objective uncertainty, Optim. Online (2018).

[61] P. Aaslid, F. Geth, M. Korpås, M.M. Belsnes, O.B. Fosso, Non-linear charge-based battery storage optimization model with bi-variate cubic spline constraints, J. Energy Storage 32 (2020) 101979, https://doi.org/10.1016/j.est.2020.101979.

[62] O.B. Fosso, M.M. Belsnes, Short-term hydro scheduling in a liberalized power system. 2004 International Conference on Power System Technology PowerCon 2004 2, 2004, pp. 1321–1326, https://doi.org/10.1109/ICPST.2004.1460206.